

# ALMA Extends to 15-kilometre Baselines: Submillimetre Science down to 20-Milliarcsecond Resolution

Catherine Vlahakis<sup>1,2</sup>  
Leonardo Testi<sup>2</sup>  
Paola Andreani<sup>2,3</sup>

<sup>1</sup> Joint ALMA Observatory, Santiago, Chile

<sup>2</sup> ESO

<sup>3</sup> ESO ALMA Regional Centre

From September to late November 2014, the Atacama Large Millimeter/submillimeter Array (ALMA) carried out a Long Baseline Campaign to test and verify baselines up to ~ 15 kilometres for the first time. The tests were successful, demonstrating the power of ALMA to produce submillimetre-wave imaging at resolutions of tens of milliarcseconds. Science Verification observations of five targets, including an asteroid, a protoplanetary disc, an evolved star and a gravitationally lensed high-redshift galaxy, were obtained. The results demonstrate that the scientific leap for which ALMA was planned has been made. A brief overview of the 2014 Long Baseline Campaign and its scientific results are presented.

ALMA is a global project with partners in Europe, North America (USA and Canada) and East Asia (Japan, Taiwan and the Republic of Korea), to build and

operate the world's largest millimetre/submillimetre array, located on the Chajnantor Plateau in the north of Chile at an elevation of 5000 metres above sea level. ALMA, inaugurated in 2013, has a full complement of 66 antennas. The Call for Proposals for Early Science Cycle 3 has recently closed, with a record number of proposals received.

A key new capability offered in Cycle 3 is observing at high angular resolution using baselines of up to ten kilometres. This mode was tested and verified during a dedicated campaign held in the last quarter of 2014. A summary of this campaign — the 2014 ALMA Long Baseline Campaign — is presented here. Activities continue to extend and upgrade the capabilities, including new receivers, digital electronics, data handling and analysis software, and new observing modes (such as millimetre-wave very long baseline interferometry), with the goal of maintaining ALMA at the forefront of astrophysical research for many decades to come.

## The 2014 ALMA Long Baseline Campaign

Imaging at resolutions of tens of milliarcseconds (mas) is a major goal of ALMA. This requires baselines of up to almost 16 kilometres, achieved using the distant

antenna stations on the Chajnantor site that have been built for this purpose, stretching out to almost ten kilometres from the centre of the array. The 2014 ALMA Long Baseline Campaign (LBC) carried out the first ever tests using these distant antenna stations; it was the first time the whole observatory infrastructure had been used for antenna separations above about three kilometres. The LBC tests were carried out from September to November 2014 and consisted of extensive testing with 23 antennas on long baselines of up to 15 kilometres, together with additional antennas on short (about 300 metres) baselines in order to provide the short spacings that are necessary for imaging extended objects. A total of 22–36 antennas were employed for the LBC tests, with the number depending on observing band; most tests were carried out in Band 3 (100 GHz). A paper (ALMA Partnership, Fomalont et al., 2015; hereafter ALMA I) provides details of the technical and calibration aspects of the LBC, and a brief summary is given here.

ALMA calibration normally uses the phase referencing observing mode, whereby short scans of the science target and a nearby quasar calibrator target are alternated over the duration of the observation, such that the phase measured on the calibrator can be transferred to the target. The accuracy with which this can be

Clem & Adri Bacri-Normier (twingforscience.com)/ESO



Figure 1. The ALMA Chajnantor site from the air in early 2013.

achieved was a critical factor for the outcome of the long baseline observations, and was addressed with a test strategy that included: a) establishing the phase coherence of the long baseline array by carrying out test observations of quasars; b) determining the observing strategy needed to achieve good imaging results; and c) carrying out Science Verification (SV) observations to demonstrate the end-to-end process from observation to calibration to imaging. In order to address the former two points, the LBC tests included:

- 1) determination of the statistics of the temporal phase variation as a function of baseline length using observations of a single bright quasar;
- 2) determination of the accuracy of the phase transfer using alternating observations of two quasars that are close together on the sky;
- 3) development of a quasi real-time method to estimate the feasibility of given long baseline observations;
- 4) determination of the optimal time interval (cycle time) between calibrator scans;
- 5) determination of antenna positions and delay model errors using observations of many quasars distributed over the sky;
- 6) flux density measurement for candidate weak phase calibrators;
- 7) investigation of potential significant structure in calibrator sources when observed at long baselines; and
- 8) measurement of the positional accuracy at long baselines, by phase referencing among many quasars that are close together on the sky.

Details of these experiments, the analysis and conclusions are described in ALMA I.

An enormous amount was learned about ALMA observing at long baselines during the highly successful LBC and some of the main results are briefly summarised here (see ALMA I for details). Further investigations are also ongoing, and additional long baseline testing will take place in the last quarter of 2015 in order to further improve the observing mode and test long baseline imaging at higher frequencies.

It was found that calibration via phase referencing should, for most sources, only be carried out when the short-

term phase root mean square (rms) is  $< 30$  degrees. The cycle time needed for phase referencing calibration to produce good image quality was found to be 60–90 seconds in almost all cases. The most reliable method of determining whether phase conditions are suitable for carrying out a given observation of a science target is with short observations of a strong quasar (the “Go/noGo” procedure), rather than predictions. The water vapour radiometer (WVR) correction, which takes into account estimated variations in the amount of precipitable water vapour along the line of sight to each antenna (see Nikolic et al., 2011; 2013), typically improves the phase noise by a factor of about two for clear skies, and further phase fluctuations are thought to be due to variations in the dry atmosphere.

The lack of an accurate dry atmospheric delay model, due to pressure variation across the array over distances of several kilometres and the current single pressure measurement at the centre of the array, is the dominant cause of systematic phase differences (longer-term variations, i.e., over timescales of minutes to hours) between observations of the phase calibrator and the science target. The addition of further weather stations in the coming months, providing several pressure measurements across the array, will allow improvement of the delay model and will be the main focus of the further long baseline testing later in 2015. It is also expected that the addition of further pressure sensors will improve the astrometric accuracy.

The survey for weak calibrators will continue in order to increase the number of sources in the ALMA calibrator catalogue (Fomalont et al., 2014). However, in order to find the faintest usable calibrators, and thereby ensure that a suitable calibrator can be found close enough to a science target, it is likely that a different observing strategy may need to be adopted in future.

For some of the SV targets (see the next section for details), the emission was sufficiently strong that it was possible to use the self-calibration technique to improve the image quality. For Juno, self-calibration provided an improvement in

the peak/image rms of a factor of two to six compared to imaging with phase referencing alone. For HL Tau, the improvement was up to a factor of two. For SDP.81, self calibration was not possible at all. Conversely, for the quasar 3C 138, which has emission that is dominated by a strong compact core and other relatively simple structures, the improvement ranged from a factor of 15 to 30. See ALMA I for further details. Thus, more sophisticated methods of self calibration may need to be implemented in future for some extended sources. Another finding from the SV imaging was that in many cases the integration time on source may be driven not by the need to reach a given signal rms, but by the need to obtain sufficient coverage of the  $uv$  (Fourier domain) plane.

#### Science Verification observations at long baselines

Continuum and spectral line observations of five SV targets were carried out to demonstrate the long baseline potential of ALMA, chosen from a broad range of science topics. The targets were the asteroid Juno, the asymptotic giant branch (AGB) star Mira, the circumstellar disc around the young star HL Tau, the quasar 3C 138, and the gravitationally lensed submillimetre galaxy SDP.81. The baselines typically ranged from 15 metres to ~ 15 kilometres, and observations were taken in two or three bands (selected from Bands 3, 4, 6 and 7). The fully verified SV datasets are publicly available on the ALMA Science Portal<sup>1</sup>.

The results of the LBC are presented in a collection of four ApJ Letters by the ALMA Partnership. A summary of the main test results and SV observations is presented in ALMA I. Initial results on the SV targets Juno, HL Tau and SDP.81 are presented in ALMA Partnership, Hunter et al. (2015; hereafter ALMA II), ALMA Partnership, Brogan et al. (2015; hereafter ALMA III) and ALMA Partnership, Vlahakis et al. (2015; hereafter ALMA IV), respectively.

#### Juno

ALMA’s combination of excellent continuum brightness sensitivity at high angular resolution and well-matched wavelength

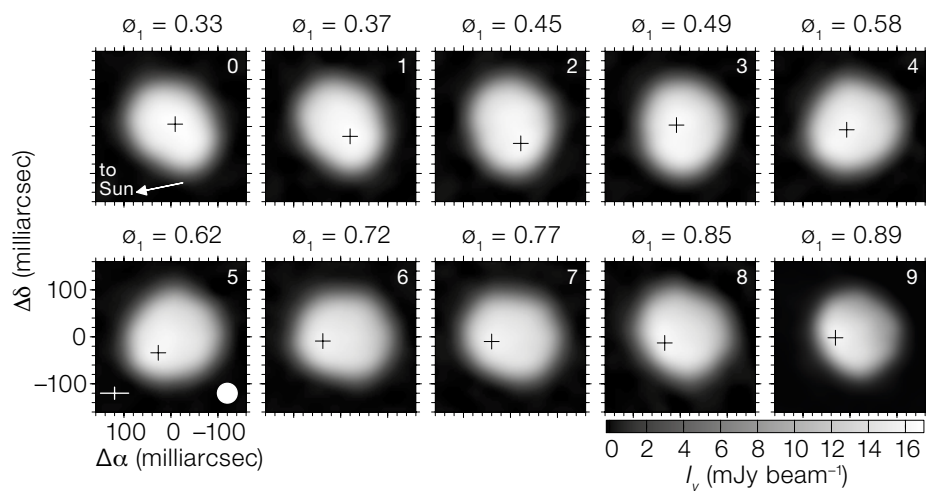


Figure 2. The sequence of ten ALMA LBC 1.3 millimetre continuum images of asteroid 3 Juno obtained over 60% of a 7.2-hour rotation, labelled by the rotation phase. The cross marks the position of peak intensity. From ALMA Partnership, Hunter et al. (2015).

coverage will enable mapping of the shape and surface temperature distribution for large numbers of main belt asteroids and Jupiter Trojans when using the full high angular resolution capability. With physical temperatures of 100–200 K, it should be possible to image these types of bodies at high signal-to-noise (S/N) at resolutions as fine as ~10 kilometres. The LBC SV observations of the asteroid 3 Juno, obtained in October 2014 in five blocks covering four hours, provided the first ground-based images to significantly resolve the surface of an asteroid at millimetre wavelengths (1.3 mm, 233 GHz). Full details can be found in ALMA II.

Juno is a member of the S-class of asteroids (stony composite of metallic iron and iron-bearing silicates). Its apparent mean diameter (from occultation studies) is 267 kilometres, although it is a triaxial ellipsoid and its rotation period is 7.21 hours. Its mean orbital radius is

2.67 astronomical units (au) and during the SV observations the illumination was 94%. Figure 2 shows the resulting ten 1.3-millimetre continuum images (two per observing block; labelled by rotational phase). The peak brightness temperature varies from 207 K to 222 K over the time sequence, with a median value of 215 K. Comparison with models of the size and shape of the asteroid from the Database of Asteroid Models from Inversion Techniques (DAMIT; Durech et al., 2010) shows good agreement (ALMA II).

While the LBC images of Juno provide a very good example of what ALMA can achieve for this asteroid at 233 GHz, observations of Juno and other main belt asteroids at shorter wavelengths would provide higher spatial resolution, e.g., ~20 kilometres at 345 GHz (Band 7) with a similar configuration when the asteroid is at a more favourable position (at a distance from Earth of ~1 au). ALMA

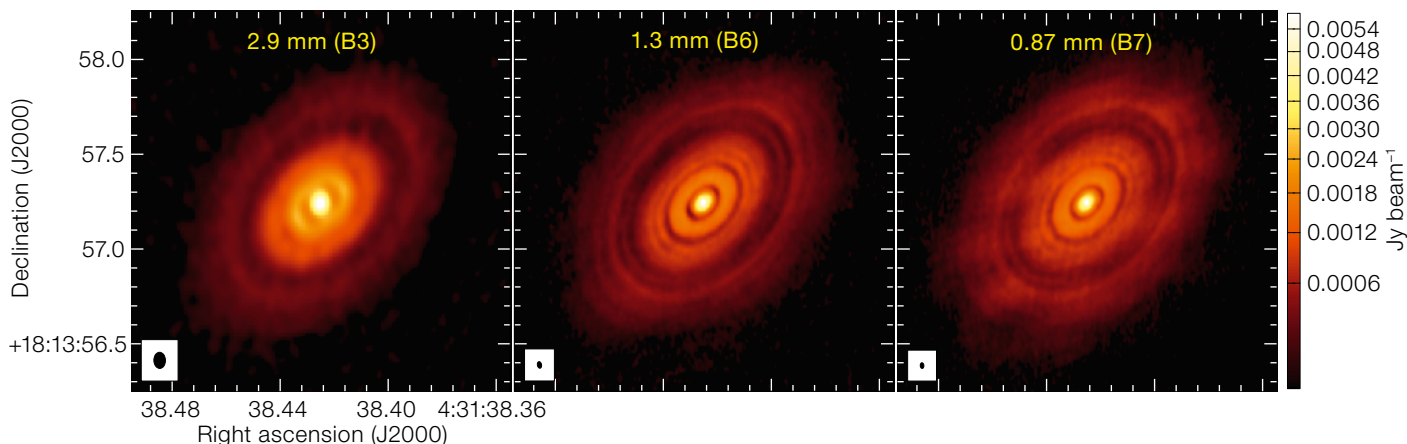
will also be able to provide improved long-term modelling of asteroid orbits, enabling improved prediction from the models, by delivering very accurate astrometry.

**The HL Tau protoplanetary disc**

The 1.3-millimetre ALMA image of HL Tau — a heavily embedded young stellar object surrounded by a protoplanetary disc — could be said to be synonymous with the success of the LBC, having been the first image to emerge from the early part of the campaign and the subject of a high-impact press release<sup>2</sup>. The image was featured on the front cover of *Messenger* 158. However, the LBC SV for this source extended beyond this initial result, with data also observed at 2.9 mm (Band 3) and 0.87 mm (Band 7), achieving even higher angular resolution at 0.87 mm (25 mas, or 3.5 au at the distance of HL Tau).

HL Tau is located within a ~0.05 pc molecular ridge in the Taurus star-forming region, which is at a distance of 140 pc. While only observed as a conical reflection nebula at optical wavelengths, due to high extinction, HL Tau has however been well observed in the near- and mid-

Figure 3. ALMA continuum images of HL Tau at 102, 233 and 344 GHz (Bands 3, 6 and 7). The beam size is shown for each image. From ALMA Partnership, Brogan et al. (2015).



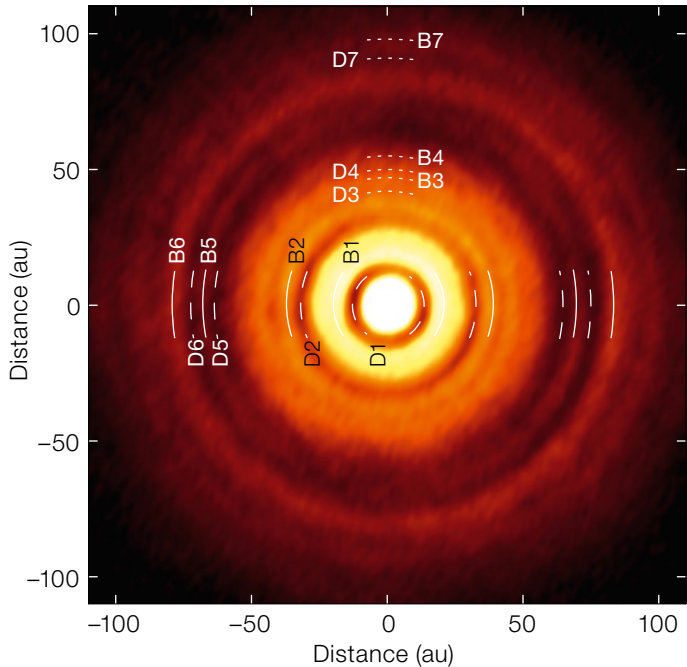


Figure 4. The deprojected 1.0 mm (287 GHz) ALMA image of the circumstellar disc around HL Tau at an angular resolution of  $39 \times 19$  mas. From ALMA Partnership, Brogan et al. (2015).

$\text{HCO}^+(1-0)$ , HCN,  $^{12}\text{CO}(1-0)$  and CN. At this resolution the HL Tau region has complex outflow emission (see ALMA III). The  $\text{HCO}^+(1-0)$  emission was also imaged at 0.25-arcsecond resolution: most of the outflow emission is resolved out, allowing the morphology of the HL Tau molecular gas disc to be spatially resolved for the first time (ALMA III).

#### The gravitationally lensed $z \sim 3$ submillimetre galaxy SDP.81

SDP.81 (HATLAS J090311.6+003906) is a  $z = 3.042$  submillimetre galaxy gravitationally lensed by an intervening elliptical galaxy at  $z = 0.299$ . SDP.81 was first detected in the *Herschel* ATLAS (H-ATLAS) survey (Negrello et al., 2010) and subsequently resolved in the millimetre continuum as well as CO and  $\text{H}_2\text{O}$  molecular line emission at 0.6–3-arcsecond resolution with the Submillimeter Array (SMA) and the Plateau de Bure Interferometer (PdBI); see Bussmann et al. (2013) and Omont et al. (2013). As part of SV for the ALMA LBC, the target was observed in Bands 4, 6 and 7: Band 4 included the CO J=5-4 line, Band 6 the CO J=8-7 and the low excitation water line  $\text{H}_2\text{O}(2_{02} - 1_{11})$  and Band 7 included the CO J=10-9 line. Full details are presented in ALMA IV.

Figure 5 shows the high resolution continuum images at Bands 4, 6 and 7, reaching angular resolutions as fine as 23 mas. This resolution is better than the Hubble Space Telescope images of this source, and corresponds to an unlensed spatial scale of  $\sim 180$  pc in the lensed galaxy, or a few tens of pc in the source plane considering a magnification factor of  $\sim 11$ –20. Viewed at this level of detail, strong detections of thermal dust emission in two incredibly thin arcs, which are the main components of an Einstein ring, were achieved. In addition to the eastern and western arcs, a continuum source was detected in all three bands at the central position of the lens (the early-type galaxy SDSS J090311.57+003906.5). This central continuum source is likely due to a weak, previously undetected, active galactic nucleus (AGN) in the foreground elliptical galaxy (see ALMA IV) and there is no evidence of a central lensed image in the molecular line data (Wong et al., 2015).

infrared; it is found to be a Class I–II protostar of spectral type around K5 with a collimated outflow. Since the HL Tau disc is one of the brightest at millimetre and submillimetre wavelengths, it has been a well-studied source since the early 1990s. The highest resolution observations prior to the ALMA LBC were obtained with the Combined Array for Research in Millimeter-wave Astronomy (CARMA) at a resolution of 0.13 arcseconds (18 au at 140 pc), which was sufficient to resolve the disc (Kwon et al., 2011).

ALMA observed HL Tau as part of the LBC in October–November 2014, using Bands 3, 6 and 7 (2.9, 1.3 and 0.87 mm, or  $\sim 100$ , 240 and 345 GHz, respectively); details of the observations and initial analysis are presented in ALMA III. Figure 3 shows the continuum images; the size of the synthesised beam for the 0.87 mm Band 7 image is an impressive  $30 \times 19$  mas. Figure 4 shows the combined Band 6 and 7 (1.0 mm) image, deprojected by the line of sight inclination of the disc of 46.72 degrees (derived from fitting each ring assuming circular orbits) with the bright and dark rings labelled (as B1–7 and D1–6, respectively). The spectral index (derived from the flux variation with wavelength across the three bands) is found to vary as a function of radial distance, with the dark rings having

a higher spectral index compared to the bright rings; rather than being entirely devoid of emission, the dark rings are likely to be optically thin. The centres of most of the rings are also found to be offset from the emission peak, making the rings non-circular, with HL Tau at one focus; the size of the offsets increases with the ring radius. Furthermore, there are apparent resonances between the radii of some of the rings.

The striking conclusion from ALMA III is that all these pieces of evidence, taken together, are highly suggestive of planet formation within the disc. Alternative interpretations have been discussed in the literature and involve grain growth promotion and trapping at specific locations in the disc, either due to instabilities or chemical/phase transitions in the gaseous component of the disc (Zhang et al., 2015). Further modelling and observations will elucidate the initial results from the LBC. The combination of high angular resolution and high fidelity imaging has already revealed a wealth of detail in the circumstellar disc, demonstrating the power of ALMA to deliver transformational science.

The HL Tau SV observations did not just include continuum emission. Four spectral lines were also imaged in Band 3, at 1.1-arcsecond angular resolution ( $\sim 25$  au):

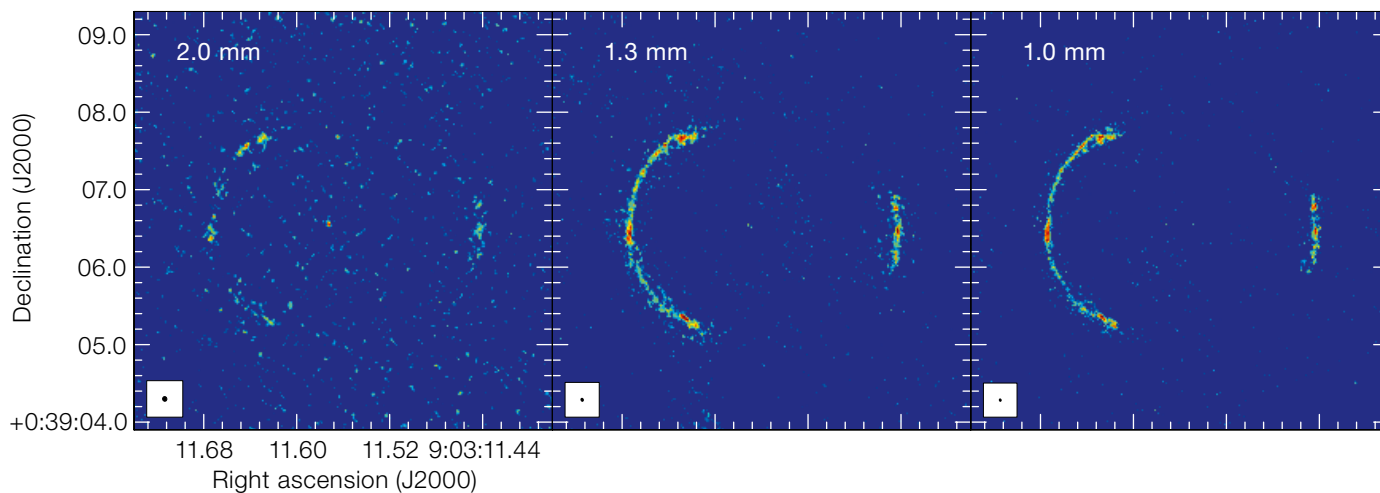
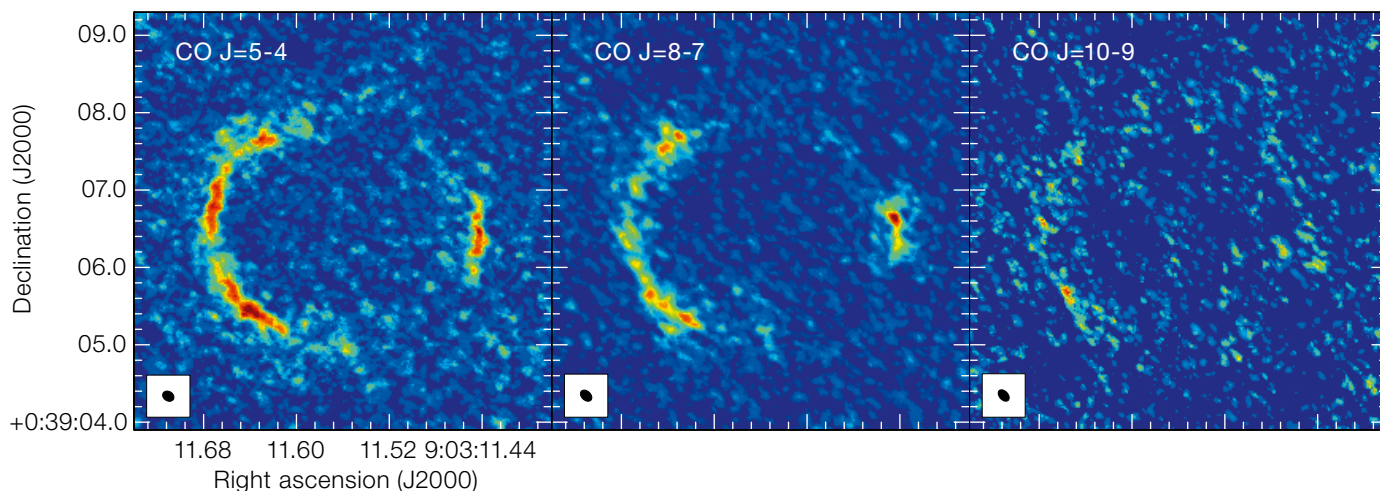


Figure 5. (Above) ALMA continuum images of the gravitationally lensed  $z \sim 3$  galaxy SDP.81 in Bands 4 (2.0 mm), 6 (1.3 mm) and 7 (1.0 mm), left to right. The highest angular resolution, at 1.0 mm (290 GHz) in Band 7, is  $31 \times 23$  mas (right panel). From ALMA Partnership, Vlahakis et al. (2015).

Figure 6. (Below) ALMA CO integrated intensity images of the gravitationally lensed  $z \sim 3$  galaxy SDP.81 in Band 4 (CO J=5-4), Band 6 (CO J=8-7) and Band 7 (CO J=10-9), from left to right. The angular resolution is  $\sim 170$  mas. From ALMA Partnership, Vlahakis et al. (2015).



The three transitions of CO (J=5-4, J=8-7 and J=10-8) were also imaged (see Figure 6). In order to achieve good S/N, the spectral lines were imaged at somewhat coarser resolution ( $\sim 170$  mas). The CO morphology is broadly similar to that seen in the continuum, tracing two main gravitational arcs; the CO emission in each arc, however, is clumpier. The spatially integrated CO line profiles show evidence of two components separated by  $\sim 300$  km  $s^{-1}$ , with the lower velocity emission occurring predominantly in the western arc. Thermal H<sub>2</sub>O line emission was clearly detected in the eastern arc and at low S/N in the western arc, but to achieve these detections only the shorter

baselines were used, giving an angular resolution of  $\sim 0.9$  arcseconds (ALMA IV). Nonetheless, with this detection at 0.9-arcsecond resolution, ALMA has achieved the highest resolution detection of thermal water emission in an extragalactic source to date. The water emission is confined to only one of the velocity components, in agreement with previous observations with the PdBI (Omont et al., 2013).

There have already been several additional studies based on the ALMA LBC observations, including one on mass modelling of the lensing elliptical at  $z = 0.299$  that suggests a stellar core of

mass-to-light ratio of  $\sim 2 M_{\odot} L_{\odot}^{-1}$ , or a  $> 3 \times 10^8 M_{\odot}$  black hole if an AGN is present (Tamura et al., 2015; Wong et al. 2015). Dye et al. (2015), Rybak et al. (2015a) and Swinbank et al. (2015) have modelled the background starburst galaxy and find a highly non-uniform distribution of dust clumps. Swinbank et al. (2015), for example, find a relatively smooth CO velocity field resembling disc-like dynamics and infer a rotating disc with a rotation velocity of 320 km  $s^{-1}$ ; they suggest a disc that is in a state of collapse, and, from comparison with HST, the data suggest a scenario where two separate systems are merging. Alternative conclusions have been presented by

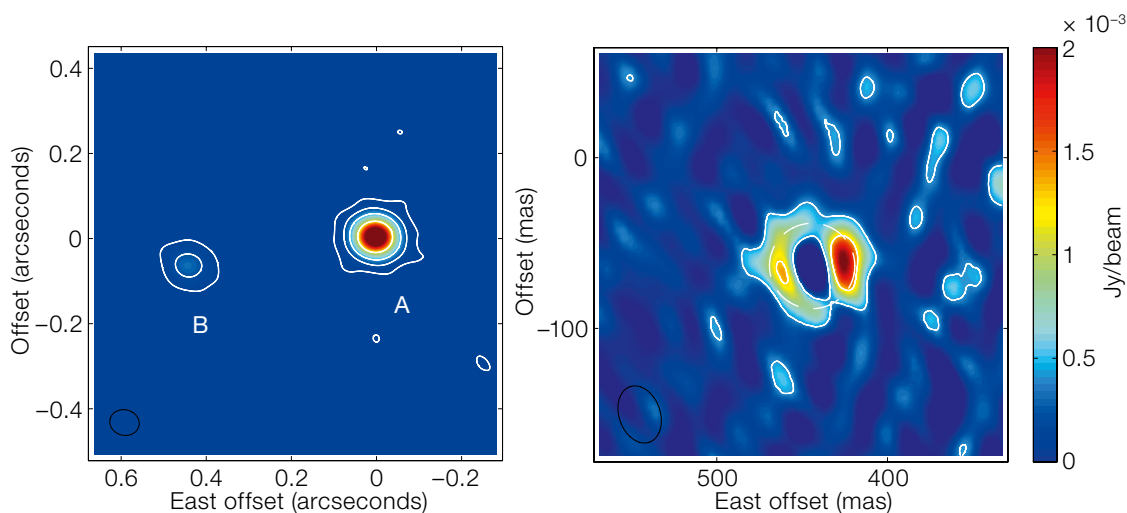


Figure 7. ALMA Band 3 image of Mira AB showing the binary (left) and the Band 6 image of Mira B with the point source subtracted, showing the partially ionised circumstellar shell (right). From Vlemmings et al. (2015).

other authors (Rybak et al., 2015b), and further analysis of the rich datasets will undoubtedly shed further light on the nature of this intriguing system.

### The evolved star Mira

The archetypal long-period variable star Mira A (o Ceti) was observed in continuum and several spectral lines in Bands 3 and 6 as part of the LBC SV. Mira A, a mass-losing AGB star, is the primary in a binary system with a companion, Mira B (VZ Ceti; thought to be a white dwarf). At a distance of 92 pc (van Leeuwen, 2007), it is the closest such binary. The Mira AB system has already been observed in the CO J=3-2 line with ALMA in Cycle 1 (Ramstedt et al., 2014) and showed indications of a complex circumstellar envelope, but the binary pair was only marginally resolved. The LBC observations have an angular resolution as fine as  $\sim 25$  mas and thus easily resolve the binary pair (see Figure 7).

Vlemmings et al. (2015) presented an analysis of the LBC SV continuum data, determining the size, shape, flux density and spectral index of both sources in the AB system. For the first time in the sub-millimetre, the extended atmosphere of a star was resolved — Mira A was resolved into an elliptical disc with a major axis of 42 mas ( $\sim 3.8$  au) at 94 GHz (Band 3) and 43 mas (4.0 au) at 229 GHz (Band 6). Brightness temperatures were found to be  $\sim 5300$  K and 2500 K, respectively in

Bands 3 and 6, with a hotspot of  $\sim 10\,000$  K brightness temperature on the stellar disc; it is suggested that the hotspot may be related to magnetic activity. A partially ionised region of  $\sim 2.4$  au diameter (26 mas) around Mira B was also resolved (Figure 7, right), and the emission is found to be consistent with material close to the Mira B accretion disc that has been gravitationally captured from the AGB wind (see Vlemmings et al. [2015] for details).

### Prospects

The ALMA LBC observations have been spectacularly successful, both in terms of reaching the high angular resolutions possible at these baselines and addressing potential atmospheric and instrumental limitations, and in terms of the quality and scientific value of the SV observations. A number of analyses have already been published based on the SV observations and more can be expected given the quality and scientific novelty of these data. As a result of the success of the LBC, the Call for Proposals for Cycle 3 included allocations for long baselines, up to ten kilometres for Bands 3, 4 and 6, and showed a very strong demand. A wealth of further exciting science can certainly be expected in the years to come as ALMA achieves its full potential for observing at very high resolution.

### References

- ALMA Partnership, Brogan, C. L. et al. 2015, *ApJL*, arXiv:1503.02649 (ALMA III)
- ALMA Partnership, Fomalont, E. B. et al. 2015, *ApJL*, arXiv:1504.04877 (ALMA I)
- ALMA Partnership, Hunter, T. R. et al. 2015, *ApJL*, arXiv:1503.02650 (ALMA II)
- ALMA Partnership, Vlahakis, C. et al. 2015, *ApJL*, arXiv:1503.02652 (ALMA IV)
- Durech, J. et al. 2011, *Icarus*, 117, 313
- Dye, S. et al. 2015, *MNRAS*, submitted, arXiv:1503.08720
- Fomalont, E. et al. 2014, *The Messenger*, 155, 19
- Kwon, W. et al. 2011, *ApJ*, 741, 3
- Negrello, M. et al. 2010, *Science*, 440, 1999
- Nikolic, B. et al. 2011, *The Messenger*, 143, 11
- Nikolic, B. et al. 2013, *A&A*, 552, A104
- Omont, A. et al. 2013, *A&A*, 551, A115
- Ramstedt, S. et al. 2014, *A&A*, 570, L14
- Rybak, M. et al. 2015a, *MNRAS*, in press, arXiv:1503.02025
- Rybak, M. et al. 2015b, *MNRAS*, submitted, arXiv:1506.01425
- Swinbank, M. et al. 2015, *ApJL*, in press, arXiv:1505.05148
- Tamura, Y. et al. 2015, *PASJ*, in press, arXiv:1503.07605
- van Leeuwen, F. 2007, *A&A*, 474, 653
- Vlemmings, W. H. T. et al. 2015, *A&A*, 577, 4
- Wong, K. C. 2015, *ApJL*, submitted, arXiv:1503.05558
- Zhang, K., Blake, G. A. & Bergin, E. A. 2015, arXiv:1505.00882

### Links

- <sup>1</sup> ALMA Science Archive LBC data: <https://almascience.eso.org/news/release-of-science-verification-data-from-the-almal-long-baseline-campaign-2>
- <sup>2</sup> LBC HL Tau Release: <http://www.eso.org/public/news/eso1436/>